Featured in Physics

Anomalies in Hadronic B Decays

Raphaël Berthiaume,[1,*] Bhubanjyoti Bhattacharya,[2,†] Rida Boumris,[1,‡] Alexandre Jean,[1,§] Suman Kumbhakar,[1,‖] and David London[1,¶]

[1]Physique des Particules, Université de Montréal, 1375 Avenue Thérèse-Lavoie-Roux, Montréal, Quebec H2V 0B3, Canada
[2]Department of Natural Sciences, Lawrence Technological University, Southfield, Michigan 48075, USA

(Received 12 December 2023; accepted 9 October 2024; published 21 November 2024)

In this Letter, we perform fits to $B \to PP$ decays, where $B = \{B^0, B^+, B_s^0\}$ and the pseudoscalar $P = \{\pi, K\}$, under the assumption of flavor SU(3) symmetry [$\mathrm{SU}(3)_F$]. Although the fits to $\Delta S = 0$ or $\Delta S = 1$ decays individually are good, the combined fit is very poor: there is a 3.6σ disagreement with the $\mathrm{SU}(3)_F$ limit of the standard model ($\mathrm{SM}_{\mathrm{SU}(3)_F}$). One can remove this discrepancy by adding $\mathrm{SU}(3)_F$-breaking effects, but 1000% $\mathrm{SU}(3)_F$ breaking is required. The above results are rigorous, group theoretically—no dynamical assumptions have been made. When one adds an assumption motivated by QCD factorization, the discrepancy with the $\mathrm{SM}_{\mathrm{SU}(3)_F}$ grows to 4.4σ.

DOI: 10.1103/PhysRevLett.133.211802

For the past 10+ years, there has been an enormous amount of interest in the semileptonic B anomalies involving the decays $b \to s\ell^+\ell^-$ ($\ell = \mu,\ e$) and $b \to c\tau^-\bar{\nu}_\tau$. Interestingly, there have also been hadronic B anomalies, but these have generally flown under the radar. The $B \to \pi K$ puzzle has been around for about 20 years (see Refs. [1,2] and references therein), but discrepancies in other sets of hadronic decays have recently been pointed out. These include the U-spin puzzle [3], three puzzles involving $B_s^0 \to K^0\bar{K}^0$ [4], and a puzzle in $B_{d,s}^0 \to K^{(*)0}\bar{K}^{(*)0}$ decay [5]. Of these four, the first three involve only $B \to PP$ decays, where $B = \{B^0, B^+, B_s^0\}$, and the pseudoscalar $P = \{\pi, K\}$. This class of B decays is the focus of our study.

In all of these puzzles, one has a set of B decays whose amplitudes are related, either by a symmetry, or simply by having the same quark-level decay. The $B \to \pi K$ puzzle involves the four decays $B^+ \to \pi^0 K^+$, $B^+ \to \pi^+ K^0$, $B^0 \to \pi^- K^+$, and $B^0 \to \pi^0 K^0$, whose amplitudes form an isospin quadrilateral. U spin relates the decays $B_{d,s}^0 \to P^\pm P'^\mp$, where P and P' are each π or K. And $B_s^0 \to K^0\bar{K}^0$ is related to $B_s^0 \to K^+K^-$ by isospin, to $B^0 \to K^0\bar{K}^0$ by U spin, and to $B^+ \to \pi^+ K^0$ by virtue of having the same quark-level decay. In each set of related decays, the puzzle arises because it is found that the measured values of the observables of all the related decays are not consistent with one another.

The key point here is that all of these $B \to PP$ decays are related to one another by flavor SU(3) symmetry [$\mathrm{SU}(3)_F$]. By performing a global fit to all the $B \to PP$ observables under the assumption of $\mathrm{SU}(3)_F$, these puzzles can be combined, and one can quantify just how well (or poorly) the data are explained by the $\mathrm{SU}(3)_F$ limit of the standard model ($\mathrm{SM}_{\mathrm{SU}(3)_F}$). Analyses of this type were done many years ago [6], using diagrams as the theoretical parameters and making dynamical assumptions in order to neglect certain diagrams. But today there are enough data that no approximations are necessary—a full $\mathrm{SU}(3)_F$ fit can be performed. There are even enough observables in the fit to quantify a number of $\mathrm{SU}(3)_F$-breaking effects. As we will see, there are serious discrepancies with the SM.

We are interested in charmless $B \to PP$ decays, which are associated with the transitions $\bar{b} \to \bar{u}u\bar{q}$ and $\bar{b} \to \bar{q}$, $q = d,\ s$. The weak Hamiltonian is [7]

$$H_W = \frac{G_F}{\sqrt{2}} \sum_{q=d,s} \left(\lambda_u^{(q)} \left[c_1 (\bar{b}u)_{V-A} (\bar{u}q)_{V-A} + c_2 (\bar{b}q)_{V-A} (\bar{u}u)_{V-A} \right] - \lambda_t^{(q)} \sum_{i=3}^{10} c_i Q_i^{(q)} \right), \quad (1)$$

where $\lambda_{q'}^{(q)} = V_{q'b}^* V_{q'q}$, $q = d,\ s$, $q' = u,\ c,\ t$. Here the c_i ($i = 1$–10) are Wilson coefficients, and $Q_i^{(q)}$ represent penguin operators of two kinds: gluonic ($i = 3$–6) and electroweak ($i = 7$–10). H_W transforms as a $\mathbf{3}_1^*$, $\mathbf{3}_2^*$, $\mathbf{6}$, or $\mathbf{15}^*$ of $\mathrm{SU}(3)_F$. The initial B is a $\mathbf{3}$ and the final state is $(\mathbf{8} \times \mathbf{8})_s = \mathbf{1} + \mathbf{8} + \mathbf{27}$. Putting these all together, charmless

*Contact author: raphael.berthiaume@umontreal.ca
†Contact author: bbhattach@ltu.edu
‡Contact author: rida.boumris@umontreal.ca
§Contact author: alexandre.jean.1@umontreal.ca
‖Contact author: suman.kumbhakar@umontreal.ca
¶Contact author: london@lps.umontreal.ca

$B \to PP$ decays are described by seven reduced matrix elements (RMEs). These are

$$\begin{aligned} \lambda_u^{(q)}\text{:}\ & A_1 = \langle \mathbf{1}||\mathbf{3}_\mathbf{1}^*||\mathbf{3}\rangle, \qquad A_8 = \langle \mathbf{8}||\mathbf{3}_\mathbf{1}^*||\mathbf{3}\rangle, \\ \lambda_t^{(q)}\text{:}\ & B_1 = \langle \mathbf{1}||\mathbf{3}_\mathbf{2}^*||\mathbf{3}\rangle, \qquad B_8 = \langle \mathbf{8}||\mathbf{3}_\mathbf{2}^*||\mathbf{3}\rangle, \\ \lambda_u^{(q)} \ \&\ \lambda_t^{(q)}\text{:}\ & R_8 = \langle \mathbf{8}||\mathbf{6}||\mathbf{3}\rangle, \qquad P_8 = \langle \mathbf{8}||\mathbf{15}^*||\mathbf{3}\rangle, \\ & P_{27} = \langle \mathbf{27}||\mathbf{15}^*||\mathbf{3}\rangle. \end{aligned} \tag{2}$$

If $\mathrm{SU}(3)_F$ is unbroken, these RMEs are the same for $\Delta S = 0$ and $\Delta S = 1$ decays. However, they can be different if $\mathrm{SU}(3)_F$-breaking effects are allowed.

The idea is then to express the amplitudes for all charmless $B \to PP$ decays in terms of these seven RMEs, and then to perform a fit. However, before doing this, we note that an equivalent description of these $\mathrm{SU}(3)_F$ amplitudes is provided by quark diagrams [8,9]. There are eight topologies, representing tree (T), color-suppressed tree (C), annihilation (A), W exchange (E), penguin (P), penguin annihilation (PA), electroweak penguin (P_{EW}) and color-suppressed electroweak penguin (P_{EW}^C) amplitudes. T, C, E, and A are associated with $\lambda_u^{(q)}$, while P_{EW} and P_{EW}^C are associated with $\lambda_t^{(q)}$. P and PA each have three pieces, related to the flavor of the up-type quark in the loop. When CKM unitarity is imposed to remove the c-quark pieces, P_{uc} and PA_{uc} are associated with $\lambda_u^{(q)}$, P_{tc} and PA_{tc} with $\lambda_t^{(q)}$. Previously, it was often customary to absorb magnitudes of CKM matrix elements into these diagrams. However, in this paper the CKM factors are kept separate.

In order to find how RMEs are related to diagrams, one has to compare the expressions for amplitudes in terms of diagrams with those in terms of RMEs [10]. The five RMEs associated with $\lambda_u^{(q)}$ are related to the six diagrams T, C A, E, P_{uc} and PA_{uc} (e.g., see Ref. [8]). These diagrams only appear in five combinations, and it is convenient to eliminate E by defining five effective diagrams:

$$\begin{aligned} &\tilde{T} \equiv T + E, \qquad \tilde{C} \equiv C - E, \qquad \tilde{A} \equiv A + E, \\ &\tilde{P}_{uc} \equiv P_{uc} - E, \qquad \widetilde{\mathrm{PA}}_{uc} \equiv PA_{uc} + E. \end{aligned} \tag{3}$$

The relations between the RMEs and these effective diagrams are as follows [11]:

$$\begin{aligned} A_1 &= \frac{1}{2\sqrt{3}}\left(-3\tilde{T} + \tilde{C} - 8\tilde{P}_{uc} - 12\widetilde{\mathrm{PA}}_{uc}\right), \\ A_8 &= \frac{1}{8}\sqrt{\frac{5}{3}}\left(-3\tilde{T} + \tilde{C} - 8\tilde{P}_{uc} - 3\tilde{A}\right), \\ R_8 &= \frac{\sqrt{5}}{4}\left(\tilde{T} - \tilde{C} - \tilde{A}\right), \\ P_8 &= \frac{1}{8\sqrt{3}}\left(\tilde{T} + \tilde{C} + 5\tilde{A}\right), \\ P_{27} &= -\frac{1}{2\sqrt{3}}\left(\tilde{T} + \tilde{C}\right). \end{aligned} \tag{4}$$

The relations between diagrams and the two RMEs associated with $\lambda_t^{(q)}$ are

$$B_1 = -\frac{4}{\sqrt{3}}\left(\frac{3}{2}PA_{tc} + P_{tc}\right), \qquad B_8 = -\sqrt{\frac{5}{3}}P_{tc}. \tag{5}$$

Finally, the electroweak penguin diagrams P_{EW} and P_{EW}^C are also related to RMEs. But since there are only seven RMEs, and since all of these are related to other diagrams (see above), P_{EW} and P_{EW}^C must be related to these other diagrams. These EWP-tree relations, which hold in the $\mathrm{SU}(3)_F$ limit, are [12–14]

$$P_{\mathrm{EW}}^{(C)} = -\frac{3}{4}\left[\frac{\Sigma_9}{\Sigma_1}(\tilde{T} + \tilde{C} \underset{(-)}{+} \tilde{A}) \underset{(-)}{+} \frac{\Delta_9}{\Delta_1}(\tilde{T} - \tilde{C} - \tilde{A})\right], \tag{6}$$

where $\Sigma_1 = c_1 + c_2$, $\Delta_1 = c_1 - c_2$, $\Sigma_9 = c_9 + c_{10}$, and $\Delta_9 = c_9 - c_{10}$. Here we have kept only the contributions from Q_9 and Q_{10} of Eq. (1). This is justified because the Wilson coefficients of the two other electroweak penguin operators Q_7 and Q_8 are tiny [7].

This shows that diagrams are equivalent to RMEs. An analysis that uses diagrams to parametrize amplitudes is therefore completely rigorous from a group-theoretical point of view. One advantage of diagrams over RMEs is that it is straightforward to work out the contribution of any diagram to a given decay amplitude. It is not necessary to compute the $\mathrm{SU}(3)_F$ Clebsch-Gordan coefficients, which can be tricky.

Another advantage is that one can estimate the relative sizes of different diagrams. For example, it has been argued that E, A, and PA are much smaller than the other diagrams because they involve an interaction with the spectator quark [8,9], and so can (often) be neglected. But this is also problematic: results that use dynamical assumptions such as this are not rigorous group theoretically. In addition, one has to worry about whether the assumptions remain valid when rescattering effects are included.

In this Letter, we make no such assumptions. The amplitudes are parametrized in terms of all the diagrams, and we perform fits to the data. The sizes of the diagrams are fixed by the data. It is only at the end that we examine the effects of adding dynamical assumptions.

There are eight $B \to PP$ decays with $\Delta S = 0$ and eight with $\Delta S = 1$. The decomposition of their amplitudes in terms of diagrams is given in Tables I and II, respectively. Diagrams for $\Delta S = 0$ and $\Delta S = 1$ processes are, respectively, written without and with primes. Of course, in the limit of perfect $\mathrm{SU}(3)_F$ symmetry, $\tilde{T}' = \tilde{T}$, etc.

Of the 16 charmless $B \to PP$ decays, 15 have been observed. Their measurements have given rise to a large number of observables (CP-averaged branching ratios or $\mathcal{B}_{CP}$, direct CP asymmetries or A_{CP}, and indirect CP asymmetries or S_{CP}). A complete list of these observables,

TABLE I. Decomposition of $\Delta S = 0$ $B \to PP$ decay amplitudes in terms of diagrams.

	$\lambda_u^{(d)}$					$\lambda_t^{(d)}$			
Decay mode	$\tilde{T}$	$\tilde{C}$	$\tilde{P}_{uc}$	$\tilde{A}$	$\widetilde{\mathrm{PA}}_{uc}$	P_{tc}	PA_{tc}	P_{EW}	P_{EW}^C
$B^+ \to \bar{K}^0 K^+$	0	0	1	1	0	1	0	0	$-\frac{1}{3}$
$B^+ \to \pi^0 \pi^+$	$-(1/\sqrt{2})$	$-(1/\sqrt{2})$	0	0	0	0	0	$-(1/\sqrt{2})$	$-(1/\sqrt{2})$
$B^0 \to K^0 \bar{K}^0$	0	0	1	0	1	1	1	0	$-\frac{1}{3}$
$B^0 \to \pi^+ \pi^-$	-1	0	-1	0	-1	-1	-1	0	$-\frac{2}{3}$
$B^0 \to \pi^0 \pi^0$	0	$-(1/\sqrt{2})$	$(1/\sqrt{2})$	0	$(1/\sqrt{2})$	$(1/\sqrt{2})$	$(1/\sqrt{2})$	$-(1/\sqrt{2})$	$-(1/3\sqrt{2})$
$B^0 \to K^+ K^-$	0	0	0	0	-1	0	-1	0	0
$B_s^0 \to \pi^+ K^-$	-1	0	-1	0	0	-1	0	0	$-\frac{2}{3}$
$B_s^0 \to \pi^0 \bar{K}^0$	0	$-(1/\sqrt{2})$	$(1/\sqrt{2})$	0	0	$(1/\sqrt{2})$	0	$-(1/\sqrt{2})$	$-(1/3\sqrt{2})$

along with their present experimental values, can be found in Table III. In terms of the theoretical parameters, the observables are defined as

$$\mathcal{B}_{CP} = F_{\mathrm{PS}}(|A|^2 + |\bar{A}|^2),$$
$$\text{where } F_{\mathrm{PS}} = \frac{\sqrt{m_B^2 - (m_{P_1} + m_{P_2})^2}\sqrt{m_B^2 - (m_{P_1} - m_{P_2})^2}S}{32\pi m_B^3 \Gamma_B},$$
$$A_{CP} = \frac{|\bar{A}|^2 - |A|^2}{|\bar{A}|^2 + |A|^2}, \qquad S_{CP} = 2\mathrm{Im}\left(\frac{q}{p}\frac{\bar{A}A^*}{|\bar{A}|^2 + |A|^2}\right). \tag{7}$$

Here A and $\bar{A}$ are the amplitudes for $B \to PP$ and its CP-conjugate process, respectively, S is a statistical factor related to identical particles in the final state, and $q/p = \exp(-2i\phi_M)$, where ϕ_M is the weak phase of B_q^0-$\bar{B}_q^0$ mixing. Note that, for the direct CP asymmetry, some experiments present the result for $C_{CP} = -A_{CP}$. In the Tables, we have added the appropriate minus signs, so that all results are for A_{CP}. Also, in the fits, S_{CP} is multiplied by η_{CP}, the CP of the final state. In general $\eta_{CP} = 1$. The only exception is the final state $\pi^0 K_S$, for which $\eta_{CP} = -1$.

Consider first $\Delta S = 0$ decays. The amplitudes are a function of 7 diagrams, corresponding to 13 unknown theoretical parameters (7 magnitudes, 6 relative strong phases). From Table III, we see that there are 15 measured observables. The amplitudes also depend on the weak phases γ, β (in B^0-$\bar{B}^0$ mixing) and ϕ_s (in B_s^0-$\bar{B}_s^0$ mixing), as well as on the CKM matrix elements involved in $\lambda_{u,t}^{(q)}$. Values for all of these quantities, including errors, are taken from the Particle Data Group (PDG) [15].

As the quantities taken from the PDG are "known," we therefore effectively have 15 equations in 13 unknowns, so we can do a fit. The fit is performed using the program `MINUIT` [18]. We find an excellent fit: the $\chi^2_{\mathrm{min}}/\mathrm{d.o.f.} = 0.35/2$, for a p value of 0.84. The $\mathrm{SM}_{\mathrm{SU(3)_F}}$ therefore has no difficulty explaining the $\Delta S = 0$ data.

Turning to $\Delta S = 1$ decays, there are again 13 unknown theoretical parameters, along with 15 measured observables (Table III), so a fit can be performed. Here the fit is slightly worse, but still perfectly acceptable: $\chi^2_{\mathrm{min}}/\mathrm{d.o.f.} = 1.8/2$, for a p-value of 0.40.

If one assumes perfect $\mathrm{SU}(3)_F$ symmetry, the diagrams in $\Delta S = 0$ and $\Delta S = 1$ decays are the same. We can

TABLE II. Decomposition of $\Delta S = 1$ $B \to PP$ decay amplitudes in terms of diagrams.

	$\lambda_u^{(s)}$					$\lambda_t^{(s)}$			
Decay mode	$\tilde{T}'$	$\tilde{C}'$	$\tilde{P}'_{uc}$	$\tilde{A}'$	$\widetilde{\mathrm{PA}}'_{uc}$	P'_{tc}	PA'_{tc}	P'_{EW}	P'^C_{EW}
$B^+ \to \pi^+ K^0$	0	0	1	1	0	1	0	0	$-\frac{1}{3}$
$B^+ \to \pi^0 K^+$	$-(1/\sqrt{2})$	$-(1/\sqrt{2})$	$-(1/\sqrt{2})$	$-(1/\sqrt{2})$	0	$-(1/\sqrt{2})$	0	$-(1/\sqrt{2})$	$-(\sqrt{2}/3)$
$B^0 \to \pi^- K^+$	-1	0	-1	0	0	-1	0	0	$-\frac{2}{3}$
$B^0 \to \pi^0 K^0$	0	$-(1/\sqrt{2})$	$(1/\sqrt{2})$	0	0	$(1/\sqrt{2})$	0	$-(1/\sqrt{2})$	$-(1/3\sqrt{2})$
$B_s^0 \to K^+ K^-$	-1	0	-1	0	-1	-1	-1	0	$-\frac{2}{3}$
$B_s^0 \to K^0 \bar{K}^0$	0	0	1	0	1	1	1	0	$-\frac{1}{3}$
$B_s^0 \to \pi^+ \pi^-$	0	0	0	0	-1	0	-1	0	0
$B_s^0 \to \pi^0 \pi^0$	0	0	0	0	$(1/\sqrt{2})$	0	$(1/\sqrt{2})$	0	0

TABLE III. Measured values of $\mathcal{B}_{CP}$, A_{CP}, and S_{CP} in $\Delta S = 0$ (upper table) and $\Delta S = 1$ (lower table) $B \to PP$ decays. The † indicates data taken from the Particle Data Group [15], the * indicates data taken from Ref. [16]. All other data are taken from HFLAV [17].

Decay	$\mathcal{B}_{CP}$ $(\times 10^{-6})$	A_{CP}	S_{CP}
$B^+ \to K^+\bar{K}^0$	1.31 ± 0.14	$0.04 \pm 0.14^\dagger$	
$B^+ \to \pi^+\pi^0$	5.59 ± 0.31	0.008 ± 0.035	
$B^0 \to K^0\bar{K}^0$	$1.21 \pm 0.16^\dagger$	0.06 ± 0.26	-1.08 ± 0.49
$B^0 \to \pi^+\pi^-$	5.15 ± 0.19	0.311 ± 0.030	-0.666 ± 0.029
$B^0 \to \pi^0\pi^0$	1.55 ± 0.16	0.30 ± 0.20	
$B^0 \to K^+K^-$	0.080 ± 0.015		
$B_s^0 \to \pi^+K^-$	$5.90^{+0.87}_{-0.76}$	0.225 ± 0.012	
$B_s^0 \to \pi^0\bar{K}^0$			
$B^+ \to \pi^+K^0$	23.52 ± 0.72	-0.016 ± 0.015	
$B^+ \to \pi^0K^+$	13.20 ± 0.46	0.029 ± 0.012	
$B^0 \to \pi^-K^+$	19.46 ± 0.46	-0.0836 ± 0.0032	
$B^0 \to \pi^0K^0$	10.06 ± 0.43	-0.01 ± 0.10	0.57 ± 0.17
$B_s^0 \to K^+K^-$	$26.6^{+3.2}_{-2.7}$	-0.17 ± 0.03	0.14 ± 0.03
$B_s^0 \to K^0\bar{K}^0$	17.4 ± 3.1		
$B_s^0 \to \pi^+\pi^-$	$0.72^{+0.11}_{-0.10}$		
$B_s^0 \to \pi^0\pi^0$	$2.8 \pm 2.8^*$		

TABLE IV. Best-fit values of the magnitudes of the diagrams in units of keV for the $\Delta S = 0$ and $\Delta S = 1$ fits, as well as for the fit with unbroken $\mathrm{SU}(3)_F$.

Fit $\Delta S = 0$	$\lvert\tilde{T}\rvert$	$\lvert\tilde{C}\rvert$	$\lvert\tilde{P}_{uc}\rvert$	$\lvert\tilde{A}\rvert$
	4.0 ± 0.5	6.6 ± 0.7	3 ± 4	6 ± 5
	$\lvert\widetilde{\mathrm{PA}}_{uc}\rvert$	$\lvert P_{tc}\rvert$	$\lvert\mathrm{PA}_{tc}\rvert$	
	0.7 ± 0.8	0.8 ± 0.4	0.2 ± 0.4	
Fit $\Delta S = 1$	$\lvert\tilde{T}'\rvert$	$\lvert\tilde{C}'\rvert$	$\lvert\tilde{P}'_{uc}\rvert$	$\lvert\tilde{A}'\rvert$
	48 ± 14	41 ± 14	48 ± 15	81 ± 28
	$\lvert\widetilde{\mathrm{PA}}'_{uc}\rvert$	$\lvert P'_{tc}\rvert$	$\lvert\mathrm{PA}'_{tc}\rvert$	
	7 ± 4	0.78 ± 0.16	0.24 ± 0.04	
	$\lvert\tilde{T}'/\tilde{T}\rvert$	$\lvert\tilde{C}'/\tilde{C}\rvert$	$\lvert\tilde{P}'_{uc}/\tilde{P}_{uc}\rvert$	$\lvert\tilde{A}'/\tilde{A}\rvert$
	12 ± 4	6.6 ± 2.2	16 ± 22	14 ± 13
	$\lvert\widetilde{\mathrm{PA}}'_{uc}/\widetilde{\mathrm{PA}}_{uc}\rvert$	$\lvert P'_{tc}/P_{tc}\rvert$	$\lvert\mathrm{PA}'_{tc}/\mathrm{PA}_{tc}\rvert$	
	10 ± 13	0.97 ± 0.52	1.3 ± 2.7	
Fit $\mathrm{SU}(3)_F$	$\lvert\tilde{T}\rvert$	$\lvert\tilde{C}\rvert$	$\lvert\tilde{P}_{uc}\rvert$	$\lvert\tilde{A}\rvert$
	4.7 ± 0.5	5.8 ± 0.6	2.1 ± 0.5	4.2 ± 0.7
	$\lvert\widetilde{\mathrm{PA}}_{uc}\rvert$	$\lvert P_{tc}\rvert$	$\lvert\mathrm{PA}_{tc}\rvert$	
	0.70 ± 0.09	1.15 ± 0.04	0.214 ± 0.018	

therefore perform a fit including all the data—we have 30 equations in 13 unknowns. But now a serious problem arises: the best fit has $\chi^2_{\mathrm{min}}/\mathrm{d.o.f.} = 43.8/17$, for a p value of 3.6×10^{-4}. This means that the data disagree with the $\mathrm{SM}_{\mathrm{SU}(3)_F}$ at the level of 3.6σ.

We stress again that no dynamical assumptions have been made regarding the diagrams. This result is completely rigorous from a group-theoretical point of view.

Note that a similar $B \to PP$ fit including η and η' mesons was performed in Ref. [19] using the formalism of Ref. [20], and a good fit was found. However, in this analysis, the diagrams P_{EW} and P^C_{EW} were allowed to vary freely; the EWP-tree relations [Eq. (6)], which hold in the $\mathrm{SU}(3)_F$ limit, were not imposed. (We confirm that, if P_{EW} and P^C_{EW} are left free in our fit, a good fit is found. However, the EWP-tree relations are badly broken.)

Now, our result raises an obvious question. We know that $\mathrm{SU}(3)_F$ is broken in the SM. What is usually quoted as evidence is the fact that $f_K/f_\pi - 1 = \sim 20\%$. That is, we naively expect $\mathrm{SU}(3)_F$-breaking effects at this level. If such effects were included, perhaps that would remove the discrepancy.

Fortunately, the fit contains enough information to address this question. Above, we found that, when one considers only $\Delta S = 0$ or $\Delta S = 1$ decays, the fits are good. In Table IV, for each fit we show the best-fit values of the magnitudes of the diagrams. In the $\mathrm{SU}(3)_F$ limit, the diagrams in $\Delta S = 0$ decays (D) are the same as those in $\Delta S = 1$ decays (D'). Thus, the ratios $|D'/D|$ provide an indication of the level of $\mathrm{SU}(3)_F$ breaking required for the SM to explain the data.

These ratios are also shown in Table IV. For the diagrams associated with $\lambda_u^{(q)}$, the average of the $|D'/D|$ central values is 11.7. For some of these ratios, the errors are large, so that the ratio is consistent with unity. However, these errors are also highly correlated: if one ratio is forced to be 1, another ratio will become even larger than its central value. The upshot is that at least one of the ratios (and probably more than one) is ~ 10.

But this corresponds to 1000% $\mathrm{SU}(3)_F$ breaking. This is obviously much larger than the $\sim 20\%$ of f_K/f_π. Thus, if the SM really does explain the data, then either the 3.5σ discrepancy is simply a statistical fluctuation (involving several different decays), or the SM breaks flavor $\mathrm{SU}(3)_F$ symmetry at an unexpectedly large level. This is the anomaly in hadronic B decays.

The large $\mathrm{SU}(3)_F$ breaking seen in the fit is actually a reflection of large $\mathrm{SU}(3)_F$ breaking in the experimental data. The present data give

$$-\frac{\delta_{CP}(B_s^0 \to K^+K^-)}{\delta_{CP}(B^0 \to \pi^+\pi^-)} = 2.90 \pm 0.69,$$
$$-\frac{\delta_{CP}(B_s^0 \to K^+K^-)}{\delta_{CP}(B_s^0 \to \pi^+K^-)} = 3.43 \pm 0.91, \tag{8}$$

where $\delta_{CP}(B_q \to PP') = A_{CP}\mathcal{B}_{CP}/F_{\mathrm{PS}}$ [see Eq. (7)]. In the $\mathrm{SU}(3)_F$ limit, both of these ratios are expected to equal 1 [21–23]. Thus, the above experimental results each indicate $\sim 300\%$ $\mathrm{SU}(3)_F$ breaking. Our analysis shows that, when all decays are examined simultaneously, the net

$SU(3)_F$-breaking effect is quite a bit larger. It is also expected that $-\delta_{CP}(B_s^0 \to K^0\bar{K}^0)/\delta_{CP}(B^0 \to K^0\bar{K}^0) = 1$ in the $SU(3)_F$ limit. This ratio has not yet been measured, but according to our analysis, it should also exhibit very large $SU(3)_F$ breaking.

The sizable width difference in the B_s^0 system, $\Delta\Gamma_s$, modifies the branching ratios of certain $B_s^0 \to f$ decays extracted from untagged samples by a correction factor involving the $\Delta\Gamma_s$-dependent CP asymmetry, $A_{\Delta\Gamma}^f$ [24]. However, $A_{\Delta\Gamma}^f$ has been measured in only one decay, $B_s^0 \to K^+K^-$. The inclusion of this correction factor increases $\mathcal{B}(B_s^0 \to K^+K^-)$ by 8%, making the $SU(3)_F$-breaking effects in Eq. (8) even larger and the fits considerably worse. Thus, it is likely that the discrepancy with the $SM_{SU(3)_F}$, and the size of SU(3)F breaking required to remove this discrepancy, are even larger than described above.

But this is not all. Up to now, the analysis has been completely rigorous, group theoretically—no dynamical assumptions were made regarding the diagrams. Returning to Table IV, we see that, although the $\Delta S = 0$ and $\Delta S = 1$ fits are good, they require values for the diagrams that are well outside theoretical expectations.

As noted earlier, it has been argued that E, A, and PA are negligible compared to the dominant diagrams [8,9]. For $\widetilde{\mathrm{PA}}$ and $\widetilde{\mathrm{PA}}'$, this is reasonably borne out by the data: $|\widetilde{\mathrm{PA}}_{uc}/\tilde{T}|$ and $|\widetilde{\mathrm{PA}}'_{uc}/\tilde{T}'|$ are both quite a bit smaller than 1. Note that, since $\widetilde{\mathrm{PA}}_{uc} \equiv PA_{uc} + E$ [Eq. (3)], technically PA_{uc} and E could both be large. But in order to obtain the small $|\widetilde{\mathrm{PA}}_{uc}|$, this would then require a fine-tuned cancellation between these two diagrams. A more natural assumption is that $|\mathrm{PA}_{uc}|$ and $|E|$ are both of the order of $|\widetilde{\mathrm{PA}}_{uc}|$. Furthermore, $|\mathrm{PA}_{tc}|$ is small. The data therefore largely confirm the theoretical expectation that E and PA are much smaller than the dominant diagrams. On the other hand, in Table IV, we see that $|\tilde{A}/\tilde{T}|$ and $|\tilde{A}'/\tilde{T}'|$ are both $O(1)$. This is very strange—why would A be large, while E and PA are small?

Another curious result is related to the ratio $|C/T|$. Naively, we expect $|C/T| = 1/3$, simply by counting colors. This expectation is borne out by theoretical calculations. In QCD factorization, this ratio is computed for $B \to \pi K$ decays ($\Delta S = 1$). It is found that $|C'/T'| \simeq 0.2$ at NLO [25], while at NNLO, $0.13 \leq |C'/T'| \leq 0.43$, with a central value of $|C'/T'| = 0.23$, very near its NLO value [26–29].

On the other hand, the fits of Table IV have $|\tilde{C}/\tilde{T}| = 1.65$ ($\Delta S = 0$), $|\tilde{C}'/\tilde{T}'| = 0.85$ ($\Delta S = 1$), and $|\tilde{C}/\tilde{T}| = 1.23$ [$SU(3)_F$]. It is true that $\tilde{T}$ and $\tilde{C}$ include contributions from E, but since E has been shown to be small, $|\tilde{C}/\tilde{T}| \simeq |C/T|$, and similarly for the primed diagrams.

If we fix $|\tilde{C}^{(\prime)}/\tilde{T}^{(\prime)}|$ to 0.2 and redo the fits, we now find that the fit of $\Delta S = 1$ decays is worse than before, but still acceptable: $\chi^2_{\mathrm{min}}/\mathrm{d.o.f.} = 6.8/3$, for a p value of 0.08. (But note that $\tilde{A}'$ is now the largest diagram in this fit, with $|\tilde{A}'/\tilde{T}'| = 1.6$.) On the other hand, the fit of $\Delta S = 0$ decays is considerably worse: $\chi^2_{\mathrm{min}}/\mathrm{d.o.f.} = 18.8/3$, for a p value of 3.1×10^{-4}, corresponding to a discrepancy with the $\mathrm{SM}_{\mathrm{SU(3)_F}}$ of 3.6σ. Finally, if one assumes perfect $SU(3)_F$ symmetry, the best fit has $\chi^2_{\mathrm{min}}/\mathrm{d.o.f.} = 55.8/18$, for a p value of 9.4×10^{-6}. The discrepancy with the $\mathrm{SM}_{\mathrm{SU(3)_F}}$ has grown to 4.4σ.

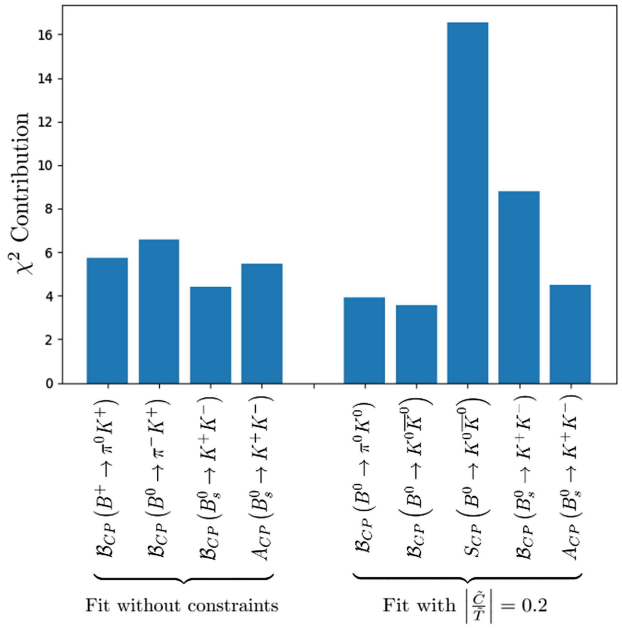

FIG. 1. Observables providing the largest χ^2 contributions for the global fits with $|\tilde{C}/\tilde{T}|$ unconstrained (left) and $|\tilde{C}/\tilde{T}| = 0.2$ (right).

As we have seen, in the global fit to both $\Delta S = 0$ and $\Delta S = 1$ decays, the discrepancy with the $\mathrm{SM}_{\mathrm{SU(3)_F}}$ is 3.6σ if $|\tilde{C}/\tilde{T}|$ is unconstrained, and it jumps to 4.4σ if $|\tilde{C}/\tilde{T}|$ is fixed to be 0.2. In Fig. 1, we identify the observables that contribute the most to the χ^2 of each of these fits. On the whole, the large-χ^2 observables are different for the two fits; the only ones that are important for both fits are the CP-averaged branching ratio and direct CP asymmetry of $B_s^0 \to K^+K^-$. This is unsurprising, given that this decay figures in both experimental results exhibiting large $SU(3)_F$ breaking [see Eq. (8)].

Note that $\Delta S = 1$ decays play a particularly important role in these discrepancies. This suggests that there may be new-physics contributions to $b \to su\bar{u}$ and $b \to sd\bar{d}$. Perhaps there is a connection with the semileptonic $b \to s\ell^+\ell^-$ anomalies.

To sum up, assuming unbroken flavor SU(3) symmetry, a global fit to all $B \to PP$ data finds a discrepancy with the $\mathrm{SM}_{\mathrm{SU(3)_F}}$ at the level of 3.6σ. This discrepancy can be removed by allowing for $SU(3)_F$-breaking effects, but 1000% $SU(3)_F$ breaking is required, i.e., parameters that are equal in the $SU(3)_F$ limit must now differ by a factor of 10. These results are group-theoretically rigorous—no dynamical assumptions have been made. But if one also

requires that $|C/T| = 0.2$, which is the predicted value in QCD factorization, the discrepancy with the $\mathrm{SM}_{\mathrm{SU(3)_F}}$ grows to 4.4σ. These are the anomalies in hadronic B decays. They strongly hint that new physics is present in these decays.

Acknowledgments—We thank Marianne Bouchard for checking the fit with the P_{EW} and P_{EW}^{C} diagrams free. This work was financially supported by NSERC of Canada (R. B., R. B., A. J., S. K., D. L.) and by the National Science Foundation, Grant No. PHY-2310627 (B. B.).

[1] N. B. Beaudry, A. Datta, D. London, A. Rashed, and J.-S. Roux, The $B \to \pi K$ puzzle revisited, J. High Energy Phys. 01 (2018) 074.

[2] B. Bhattacharya, A. Datta, D. Marfatia, S. Nandi, and J. Waite, Axion-like particles resolve the $B \to \pi K$ and $g-2$ anomalies, Phys. Rev. D **104**, L051701 (2021).

[3] B. Bhattacharya, S. Kumbhakar, D. London, and N. Payot, U-spin puzzle in B decays, Phys. Rev. D **107**, L011505 (2023).

[4] Y. Amhis, Y. Grossman, and Y. Nir, The branching fraction of $B_s^0 \to K^0 \bar{K}^0$: Three puzzles, J. High Energy Phys. 02 (2023) 113.

[5] A. Biswas, S. Descotes-Genon, J. Matias, and G. Tetlalmatzi-Xolocotzi, A new puzzle in non-leptonic B decays, J. High Energy Phys. 06 (2023) 108.

[6] C.-W. Chiang, M. Gronau, J. L. Rosner, and D. A. Suprun, Charmless $B \to PP$ decays using flavor SU(3) symmetry, Phys. Rev. D **70**, 034020 (2004).

[7] G. Buchalla, A. J. Buras, and M. E. Lautenbacher, Weak decays beyond leading logarithms, Rev. Mod. Phys. **68**, 1125 (1996).

[8] M. Gronau, O. F. Hernandez, D. London, and J. L. Rosner, Decays of B mesons to two light pseudoscalars, Phys. Rev. D **50**, 4529 (1994).

[9] M. Gronau, O. F. Hernandez, D. London, and J. L. Rosner, Electroweak penguins and two-body B decays, Phys. Rev. D **52**, 6374 (1995).

[10] D. Zeppenfeld, SU(3) relations for B meson decays, Z. Phys. C **8**, 77 (1981).

[11] We note that A_1, R_8 and P_8 have the opposite sign in Ref. [8]. This is simply a different convention and has no physical importance.

[12] M. Neubert and J. L. Rosner, New bound on gamma from $B^{\pm} \to \pi K$ decays, Phys. Lett. B **441**, 403 (1998).

[13] M. Neubert and J. L. Rosner, Determination of the weak phase gamma from rate measurements in $B^{\pm} \to \pi K, \pi\pi$ decays, Phys. Rev. Lett. **81**, 5076 (1998).

[14] M. Gronau, D. Pirjol, and T.-M. Yan, Model independent electroweak penguins in B decays to two pseudoscalars, Phys. Rev. D **60**, 034021 (1999); **69**, 119901(E) (2004).

[15] R. L. Workman *et al.* (Particle Data Group), Review of particle physics, Prog. Theor. Exp. Phys. **2022**, 083C01 (2022).

[16] J. Borah *et al.* (Belle Collaboration), Search for the decay $B_s^0 \to \pi^0\pi^0$ at Belle, Phys. Rev. D **107**, L051101 (2023).

[17] Y. Amhis *et al.*, Averages of b-hadron, c-hadron, and τ-lepton properties as of 2021, Phys. Rev. D **107**, 052008 (2023).

[18] F. James and M. Roos, Minuit: A system for function minimization and analysis of the parameter errors and correlations, Comput. Phys. Commun. **10**, 343 (1975); F. James and M. Winkler, MINUIT user's guide (2004), https://cds.cern.ch/record/2296388; F. James, MINUIT Function Minimization and Error Analysis: Reference Manual Version 94.1 (1994), https://zenodo.org/records/13923658; H. Dembinski, P. Ongmongkolkul *et al.*, scikit-hep/iminuit, 10.5281/zenodo.3949207 (2020).

[19] T. Huber and G. Tetlalmatzi-Xolocotzi, Estimating QCD-factorization amplitudes through SU(3) symmetry in $B \to PP$ decays, Eur. Phys. J. C **82**, 210 (2022).

[20] X.-G. He and W. Wang, Flavor SU(3) topological diagram and irreducible representation amplitudes for heavy meson charmless hadronic decays: Mismatch and equivalence, Chin. Phys. C **42**, 103108 (2018).

[21] In fact, the second ratio is predicted to equal 1 only if the $\widetilde{\mathrm{PA}}$ diagram is neglected (see Ref. [3]). But since the data show that $\widetilde{\mathrm{PA}}$ is much smaller than the other diagrams (see Table IV), this is a good approximation.

[22] Y. Grossman, Z. Ligeti, and D. J. Robinson, More flavor SU(3) tests for new physics in CP violating B decays, J. High Energy Phys. 01 (2014) 066.

[23] M. Gronau, U-spin breaking in CP asymmetries in B decays, Phys. Lett. B **727**, 136 (2013).

[24] K. De Bruyn, R. Fleischer, R. Knegjens, P. Koppenburg, M. Merk, and N. Tuning, Branching ratio measurements of B_s decays, Phys. Rev. D **86**, 014027 (2012).

[25] M. Beneke, G. Buchalla, M. Neubert, and C. T. Sachrajda, QCD factorization in $B \to \pi K, \pi\pi$ decays and extraction of Wolfenstein parameters, Nucl. Phys. **B606**, 245 (2001).

[26] G. Bell, NNLO vertex corrections in charmless hadronic B decays: Imaginary part, Nucl. Phys. **B795**, 1 (2008).

[27] G. Bell, NNLO vertex corrections in charmless hadronic B decays: Real part, Nucl. Phys. **B822**, 172 (2009).

[28] M. Beneke, T. Huber, and X.-Q. Li, NNLO vertex corrections to non-leptonic B decays: Tree amplitudes, Nucl. Phys. **B832**, 109 (2010).

[29] G. Bell, M. Beneke, T. Huber, and X.-Q. Li, Two-loop current-current operator contribution to the non-leptonic QCD penguin amplitude, Phys. Lett. B **750**, 348 (2015).